JOURNAL OF CATALYSIS 60, 316–324 (1979)

Surface Chemistry of Cyanogen on Pt(111): Isotopic Exchange and Coadsorption with CO

W. HOFFMANN, E. BERTEL, AND F. P. NETZER

Institut für Physikalische Chemie, Universität Innsbruck, A-6020 Innsbruck, Austria

Received January 23, 1979; revised April 24, 1979

The adsorption of C_2N_2 on Pt(111) has been studied by thermal desorption mass spectrometry using $^{12}C_2{}^{14}N_2$ and $^{13}C_2{}^{15}N_2$ under various adsorption conditions and by work function measurements. Thermal desorption spectra revealed three desorption peaks (α, β_1, β_2) in close agreement with results on other Pt single crystal surfaces. No isotopic exchange was observed in the α peak and it is attributed therefore to molecularly adsorbed C_2N_2. Isotopic exchange between coadsorbed $^{12}C_2{}^{14}N_2$ and $^{13}C_2{}^{15}N_2$ was found in the β peaks depending on the experimental conditions. Whereas the β_2 state showed isotopic exchange irrespective of simultaneous or consecutive adsorption of $^{12}C_2{}^{14}N_2$ and $^{13}C_2{}^{15}N_2$, no isotopic exchange was detected after consecutive adsorption in the β_1 state once preformed at the surface. These results are discussed in terms of dissociative adsorption of C_2N_2 yielding CN particles into the β_2 state and of the association of CN units into a more complex adsorbate layer (β_1) at higher adsorbate densities. An overall work function increase was observed during C_2N_2 adsorption yielding $\Delta\Phi = 370$ mV at saturation. An opposite surface dipole is suggested for the α and β states. Coadsorption of C_2N_2 and CO was followed by thermal desorption and work function measurements. Whereas the C_2N_2-saturated Pt(111) surface can accommodate a considerable amount of CO, CO preadsorption drastically reduces the subsequent C_2N_2 uptake. The results indicate no reaction and little interaction between C_2N_2 and CO in the mixed adlayer.

1. INTRODUCTION

The adsorption and surface reactivity of cyanogen on Pt single crystal surfaces has been studied previously by various authors using numerous surface-sensitive techniques (*1–8*). A general feature of the adsorption of cyanogen on platinum surfaces is the relative insensitivity to the structure of the underlying metal surface, as indicated by the qualitatively similar results which have been obtained on the various Pt single-crystal surfaces. This suggests that localized metal–adsorbate interactions play a less significant role in the formation and structure of the adsorbate layer than adsorbate–adsorbate interactions. The absence of any ordered overlayers as detected by LEED should be mentioned in this context. Thermal desorption spectroscopy revealed an interesting three-peak desorption spectrum with peculiar kinetic behavior of the so-called β peaks which appear between 600 and 900°K. Accordingly, somewhat different interpretations have been favored by the various authors. Lambert and co-workers (*2*, *4*) assume an adsorbate layer of repulsively interacting CN particles to account for the existence of the β_1 and β_2 peaks in the desorption spectra, whereas Netzer *et al.* (*3*, *5*, *6*, *8*) suggest association of CN particles into a complex adsorbate layer at higher ad-

0021-9517/79/140316-09$02.00/0

sorbate densities. Electron spectroscopic observations seem to lend some support to the ideas of a more complex, associated adsorbate layer (*5–7*). As desorption from the adsorbed cyanogen layer takes place exclusively in molecular form, i.e., as C_2N_2, it should be possible to gain further insights into the surface chemistry of cyanogen on Pt by isotopic exchange measurements involving ^{13}C- and ^{15}N-labeled cyanogen.

In the present paper we report results of an isotopic exchange study using $^{13}C^{15}N$-enriched cyanogen in combination with "normal" $^{12}C^{14}N$ cyanogen in thermal desorption experiments on a Pt(111) surface. The adsorption of cyanogen on a Pt(111) surface has not been studied in previous investigations. In order to investigate changes in the density of the adsorbate layer induced by the presence of a nonreacting gas (*4*), the coadsorption of cyanogen with CO was studied by thermal desorption and work function measurements. Auger spectroscopy was used throughout the experiments to ascertain surface cleanliness. Some preliminary LEED experiments were performed and showed that on Pt(111), just as on other Pt single-crystal faces, no ordered cyanogen overlayer is formed between 170°K and the desorption temperature.

2. EXPERIMENTAL

Experiments were carried out in a stainless-steel UHV system set up for adsorption studies on single-crystal metal surfaces. The experimental arrangement has been described elsewhere (*8*, *9*). A quadrupole mass spectrometer was used for thermal desorption mass spectrometry and the related isotopic exchange measurements. As the mass spectrometer to crystal distance during this study was much larger than in our previous investigations (see, e.g., Ref. *8*) no absolute coverage values will be derived from the areas below flash desorption curves. Work function changes were recorded with a Kelvin vibrator using a tin oxide-coated stainless-steel gauze as reference electrode.

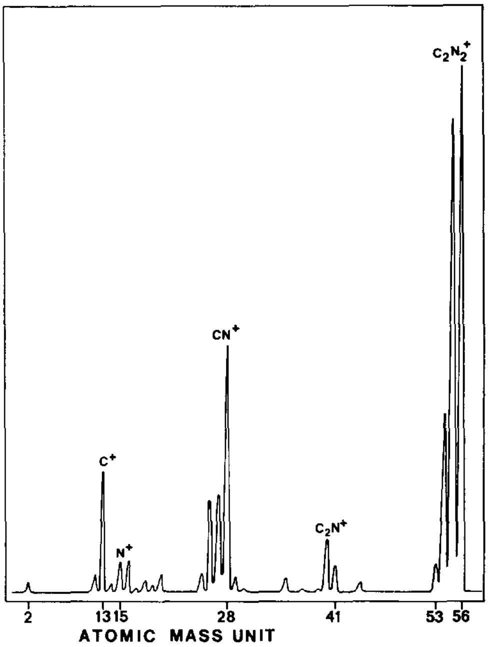

FIG. 1. Mass spectrum of $(C_2N_2)^*$ at 1.3×10^{-6} Pa (1 Pa = 7.5×10^{-3} Torr).

Cyanogen was generated by thermal decomposition of AgCN in glass cells, which were attached to the UHV chamber via leak valves. Two C_2N_2 sources were used during this study: (i) A source yielding "normal" $^{12}C_2{}^{14}N_2$ which contains in the mass spectrum beside atomic mass unit (AMU) 52 a small amount of AMU 53 originating from the natural isotope distribution (*3*). (ii) A source filled with AgCN enriched with ^{13}C and ^{15}N which was prepared from 91% ^{13}C and 95% ^{15}N KCN (Amersham–Buchler, Braunschweig, West Germany) (*10*). The resulting cyanogen, designated as $(C_2N_2)^*$, had a somewhat different isotope distribution due to the statistics in the formation process and a mass spectrum of gaseous $(C_2N_2)^*$ is shown in Fig. 1. We note beside AMU 56 the presence of AMU 55, 54 and to a small extent of AMU 53. Unfortunately, the atomic mass units expected to be formed

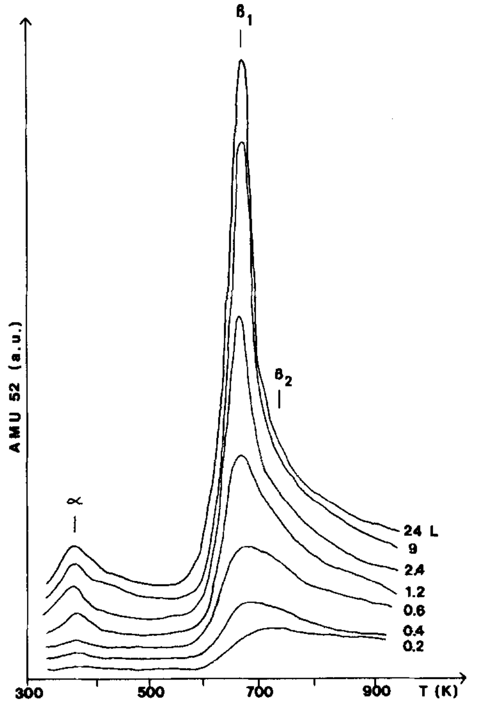

FIG. 2. Thermal desorption spectra of C_2N_2 adsorbed on Pt(111) at room temperature as a function of exposure (1 L = 10^{-6} Torr sec). Heating rate 20°K/sec.

by eventual isotopic exchange of (CN–CN) with (CN*–CN*) at the surface are already present in gaseous $(C_2N_2)^*$ and we will rely therefore on comparisons of relative intensities of AMUs in the desorption spectra to detect isotopic exchange.

The Pt(111) crystal was prepared and cleaned by standard procedures and was characterized by a sharp (1 × 1) LEED pattern (*9*).

3. RESULTS

Thermal desorption spectra of C_2N_2 (AMU 52) adsorbed on Pt(111) at room temperature are shown in Fig. 2 as a function of exposure. The α peak is observed around 370°K, the region of the β peaks extends from 600 to 850°K with the sharp β_1 peak maximum at higher surface coverages at 670°K and a β_2 shoulder around 740 to 780°K. As evident from Fig. 2 the β_2 peak is difficult to localize and its position has been determined approximately by desorption following adsorption experiments at elevated temperature (onset temperature of the β_1 peak) where the β_2 peak persists solely in the desorption spectrum. The dominant feature of the spectra is the build-up of the sharp β_1 peak with increasing surface coverage. Comparing the thermal desorption curves of C_2N_2 on Pt(111) with those on Pt(100) (*3*) and Pt-S-[9(111) × (111)] (*8*) reveals good agreement as already mentioned in Section 1. The α peak seems somewhat less populated on Pt(111) than on the other Pt surfaces. Due to a different crystal suspension in this study, the shape of the α peak is somewhat affected by partial overlapping with desorption from the suspension.

Analysis of the desorption spectra in terms of kinetic desorption parameters has to cope with the fact that the true shape of the α and especially of the β_2 peak could not be reproducibly extracted from the experimental data. Although flash desorption experiments following adsorption at elevated temperatures and isothermal desorption experiments definitely proved the existence of a β_2 peak, detailed analysis of the β_2 peak shape was not undertaken in view of the above-mentioned problems. We have mainly concentrated therefore in analyzing the β_1 peak. No shift of the β_1 peak maximum is observed with increasing surface coverage and first- or pseudo-first-order desorption kinetics with constant desorption energy seems indicated. On this basis, analysis using the peak maximum temperature (*11*) in combination with the peak width (*12*) yields a desorption energy of 190 kJ/mol and frequency factors of 10^{13}–10^{14}. On the basis of a more accurate curve fitting procedure best fit with the experimental curve shape was obtained for a desorption energy of 170 kJ/mol.

Taking the areas below the desorption curves as a measure of relative surface

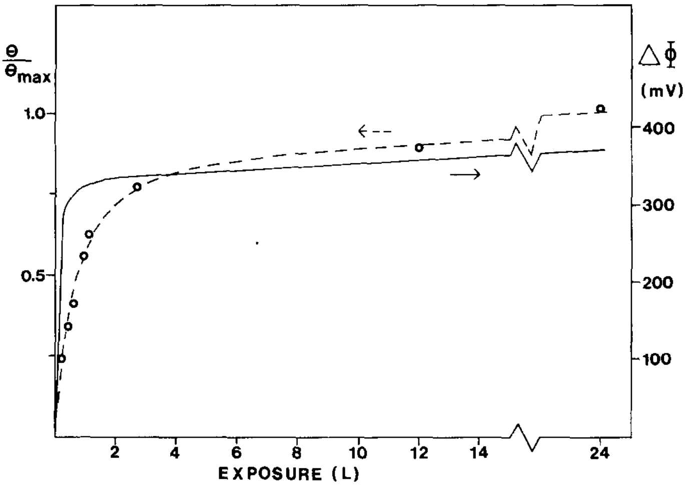

FIG. 3. C_2N_2 uptake curve derived from desorption data (O) and $\Delta\Phi$ as a function of C_2N_2 dose.

coverage the cyanogen uptake curve shown in Fig. 3 can be derived. Assuming an initial sticking probability near unity, which has been reported on other Pt surfaces (*3*, *4*), the cyanogen saturation coverage can be estimated to about 3×10^{14} molecules/cm^2. Work function changes as a function of C_2N_2 dosage are included in Fig. 3. At saturation a work function increase of 370 mV is observed. We note the difference to the flash desorption uptake curve, i.e., saturation is reached at lower C_2N_2 exposures. This can be attributed to the combined effects of depolarization within the adsorbate layer and of the opposite direction of the α and β state surface dipoles (see below and Ref. *8*).

Isotopic Exchange

The isotopic exchange experiments described in this Section were performed to investigate the formation of (CN–CN*) in the desorption process from an adsorbate layer containing both C_2N_2 and $(C_2N_2)^*$ under various experimental conditions. If the β peaks are due to associative desorption of randomly adsorbed, repulsively interacting CN particles, we would expect considerable isotopic mixing of CN and CN* in the desorption product irrespective of simultaneous or consecutive adsorption of C_2N_2 and $(C_2N_2)^*$, provided that saturation adsorption conditions were not yet established by the first adsorbate. If, on the other hand, the β_1 peak is due to desorption from an associated, polymeric-like adsorbate layer, isotopic mixing should not occur in the β_1 peak after consecutive adsorption once the β_1 state has been formed at the surface. The β_2 peak, which is thought to originate from association of individual CN particles at lower adsorbate densities, should show isotopic mixing in any case.

Isotopic exchange of adsorbed C_2N_2 with $(C_2N_2)^*$ in the gas phase was not observed. In Fig. 4 we present thermal desorption spectra of AMU 52 to AMU 56 recorded after consecutive adsorption of 0.9 L C_2N_2 and 12 L $(C_2N_2)^*$. Figure 4a shows the desorption spectrum of AMU 52 after adsorption of 0.9 L C_2N_2. A dose of 0.9 L corresponding to $\theta/\theta_{max} \approx 0.6$ was chosen for the first adsorbate to assure the existence of a β_1 state and to leave enough accessible surface for the subsequent adsorption. In Fig. 4b AMU 52 was recorded after consecutive adsorption of 12 L $(C_2N_2)^*$ to previously adsorbed 0.9 L C_2N_2. A comparison with curve a reveals

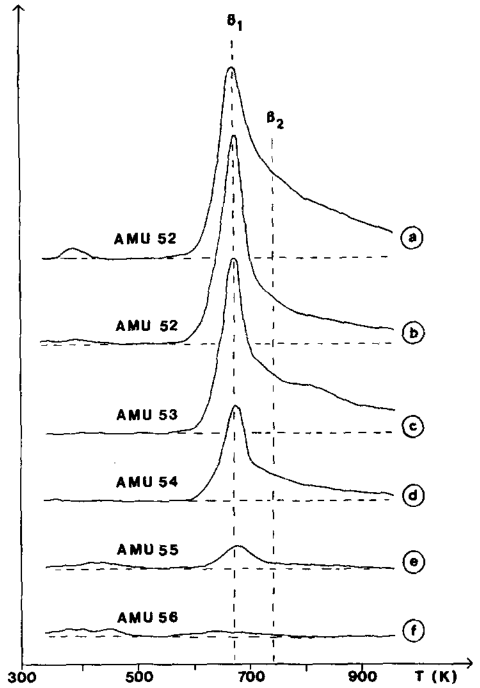

FIG. 4. Thermal desorption spectra of AMU 52–56, room temperature adsorption. (a) 0.9 L C_2N_2. (b)–(f) 0.9 L C_2N_2 followed by 12 L $(C_2N_2)^*$. Heating rate 20°K/sec.

that the β_1 peak remains unchanged whereas some depletion occurs in the β_2 peak. This suggests that isotopic exchange takes place in the β_2 state but not in the β_1 state. Curves c–f show that isotopic exchange has occurred (compare relative intensities with those in Fig. 1) but a distinction between exchange in the β_1 and β_2 state is not easily possible. Regarding the occurrence of β_1 in these spectra, it has to be kept in mind that the β_2 state originating from C_2N_2 can form β_1 with $(C_2N_2)^*$ and that, on the other hand, AMU 53 and AMU 54 are already present in the gas phases.

In order to check isotopic exchange in the β_2 state, adsorption experiments were performed at 640°K where only the β_2 state is populated. Figure 5a shows desorption of AMU 52 after adsorption of 12 L C_2N_2 at 640°K. Figures 5b and c show corresponding spectra after simultaneous and consecutive adsorption of 12 L C_2N_2 and 12 L $(C_2N_2)^*$ at 640°K. We note the decrease of the AMU 52 signal due to isotopic exchange. The fact that isotopic exchange takes place although the β_2 state is fully populated leads to the assumption that due to a high local C_2N_2 density at the surface during the subsequent exposure some β_2-C_2N_2 is shifted into the β_1 state from where it desorbs immediately at 640°K. The resulting "free β_2 sites" can then be filled with β_2-$(C_2N_2)^*$. The following experiment can be cited in support for this assumption: The surface was saturated with C_2N_2 at 640°K, cooled to 300°K after pumping-down, and then exposed to 18 L $(C_2N_2)^*$. The resulting AMU 52 desorption spectrum is shown in Fig. 5d. The decrease of the total area below the desorption curve as compared with Fig. 5a indicates isotopic exchange and the appearance of the β_1 peak due to increased adsorbate density is evident. Curves e and f in Fig. 5 correspond to the experimental

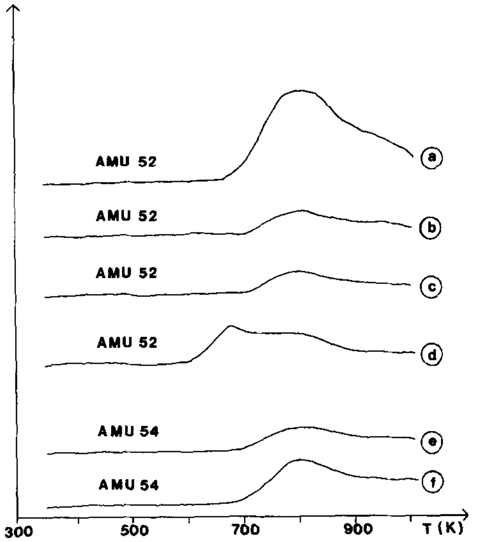

FIG. 5. Thermal desorption spectra after adsorption of (a) 12 L C_2N_2 at 640°K, (b) 12 L C_2N_2 + 12 L $(C_2N_2)^*$ simultaneously at 640°K, (c) 12 L C_2N_2 followed by 12 L $(C_2N_2)^*$ at 640°K, (d) 12 L C_2N_2 at 640°K + 18 L $(C_2N_2)^*$ at 300°K, (e) 12 L $(C_2N_2)^*$ at 640°K, (f) 12 L $(C_2N_2)^*$ + 12 L C_2N_2 simultaneously at 640°K. Heating rate 20°K/sec.

conditions of curves a and b and show the increase of AMU 54 intensity due to isotopic exchange.

Further experiments at room temperature demonstrated that isotopic exchange is observed in the β_1 state, too, if the surface is exposed simultaneously to C_2N_2 and $(C_2N_2)^*$. Less attention was paid to the α state in this investigation, but isotopic exchange can be excluded under any experimental conditions.

Briefly summarizing the results of the isotopic exchange experiments: (i) The β_1 state shows no isotopic exchange once preformed at the surface. (ii) Isotopic exchange is observed in the β_2 state. (iii) The β_1 state is populated via the β_2 state. (iv) The α state shows no isotopic exchange. These results and possible implications on the nature of the adsorbate complexes will be discussed further in Section 4.

Coadsorption with CO

The coadsorption experiments of C_2N_2 with CO reported here revealed that no chemical reactions occur between coadsorbed particles within the mixed adlayer. Similar results have been reported by Bridge and Lambert on Pt(110) (*4*). Contrary to these authors we find in this study that the energetics of both coadsorbates is almost unaffected by the coadsorbate as far as thermal desorption evidence is concerned. Figure 6 demonstrates this for the β_2 state. Curve a represents a desorption spectrum (AMU 52) after adsorption of 12 L C_2N_2 at 640°K. Curves b were recorded after exposure to 12 L C_2N_2 at 640°K, cooling to 300°K after pumping-down, and subsequent exposure to 20 L CO at 300°K. The two AMU 52 curves are almost identical and no interactions between adsorbed C_2N_2

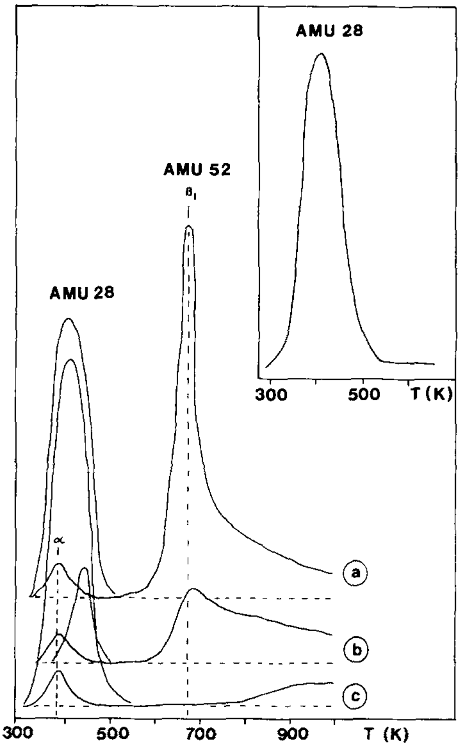

FIG. 7. Thermal desorption spectra of C_2N_2 and CO recorded after various coadsorption conditions at room temperature. (a) 50 L C_2N_2 followed by 50 L CO. (b) 0.3 L CO followed by 24 L C_2N_2. (c) 50 L CO followed by 50 L C_2N_2. The inset shows desorption of CO from the CO saturated Pt(111) surface. Heating rate 20°K/sec.

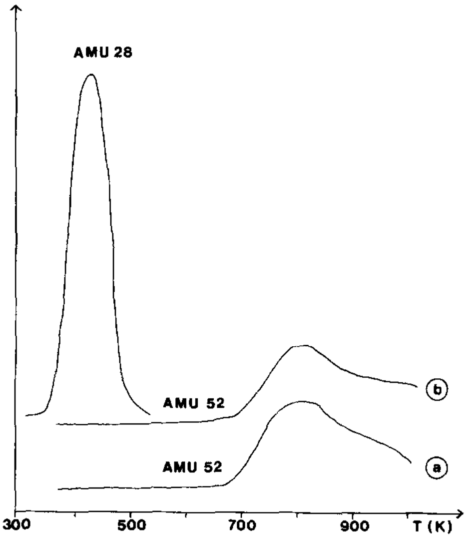

FIG. 6. Thermal desorption spectra of C_2N_2 and CO. (a) 12 L C_2N_2 at 640°K. (b) 12 L C_2N_2 at 640°K + 20 L CO at 300°K. Different sensitivity settings for AMU 28 and AMU 52. Heating rate 20°K/sec.

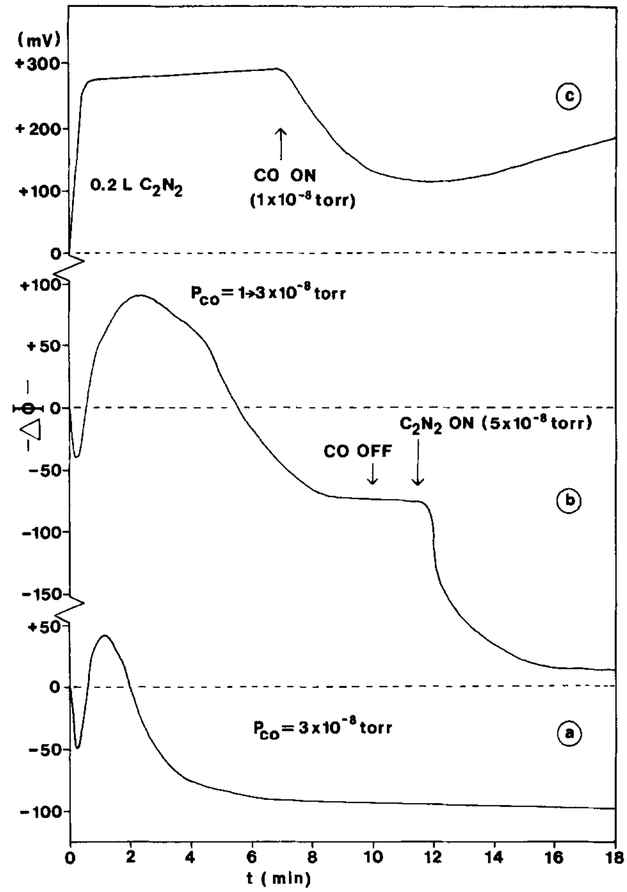

FIG. 8. Variations of the work function $\Delta\Phi$ with time. (a) At $p_{CO} = 3 \times 10^{-8}$ Torr. (b) At slightly increasing CO pressure from 1 to 3×10^{-8} Torr followed by 5×10^{-8} Torr C_2N_2. (c) During C_2N_2 uptake (~0.2 L) followed by 1×10^{-8} Torr CO stationary pressure.

and CO can be deduced. The inset in Fig. 7 shows a thermal desorption spectrum of CO from Pt(111). There is good agreement with spectra published by Ertl *et al.* (*13*). In Figs. 7a, b, and c, desorption spectra of C_2N_2 (AMU 52) and CO (AMU 28) adsorbed under various coadsorption conditions are displayed. Note the different sensitivity settings for the AMU 52 and AMU 28 spectra. In Fig. 7a 50 L C_2N_2 exposure at 300°K was followed by 50 L CO. Although the surface was saturated with C_2N_2 a considerable amount of CO corresponding to about 70% of the CO saturation value is taken up. The shape of the desorption curves again suggests no interaction. CO preadsorption, however, strongly reduces subsequent C_2N_2 adsorption (Fig. 7b). If the surface is saturated with CO, C_2N_2 can be accommodated only into the α state (Fig. 7c). This is not surprising if the saturation coverage of CO on Pt(111) at room temperature ($\theta = 0.5$) and the corresponding c (4×2) LEED structure are considered (*13*). The overproportional reduction of the amount of β-C_2N_2 by preadsorbed CO (Fig. 7b) suggests that the initial adsorption step for the incorporation of C_2N_2 into the β states, which is likely to be dissociation into CN particles, is suppressed.

Variations of the work function were recorded during coadsorption of C_2N_2 and CO on Pt(111) and are presented in Fig. 8

as $\Delta\Phi$ versus time plots. In Fig. 8a we show the variation of the work function with continuous CO uptake. There is good qualitative agreement between curve 8a and a similar $\Delta\Phi$ curve reported by Ertl *et al.* (*13*) for CO on Pt(111). Depending on the specific adsorption conditions such as different stationary CO pressure we observe quantitative changes in this curve as also noticed by Ertl *et al.* For a discussion of this rather peculiar work function behavior during CO uptake we refer to Ref. (*13*). In Fig. 8b CO uptake was followed by C_2N_2 exposure. Contrary to C_2N_2 adsorption on the bare Pt(111) surface (Fig. 3) a further work function decrease is observed here. As the α state of C_2N_2 is mainly populated under these conditions (cf. Fig. 7c), this effect could be attributed to a work function reducing character of α-C_2N_2. However, the coadsorbed α-C_2N_2 might also influence the relative distribution of CO located in bridging and on-top sites, which are thought to exhibit different surface dipoles (*13*, *14*), and more complex changes within the adsorbate layer could therefore be indicated. If C_2N_2 is preadsorbed on Pt(111), subsequent CO exposure reduces the initial work function increase and a broad minimum of $\Delta\Phi$ is observed during CO uptake of the C_2N_2 covered surface (Fig. 8c). This could be due to the subsequent filling of on-top and bridge positions by CO in a similar way as it has been rationalized upon adsorption of CO on the bare Pt(111) surface (*13*, *14*). On the other hand, more subtle interactions within the mixed adlayer, which cannot be revealed in thermal desorption experiments, could show up in work function measurements.

4. DISCUSSION

In this section we will discuss how the results presented in Section 3 can help in understanding the adsorption–desorption behavior of C_2N_2 on Pt single-crystal surfaces and whether it is possible to specify the molecular nature of the various adsorbate complexes. Previous work in this laboratory (*3*) and by Lambert *et al.* (*2*, *4*) on the adsorption of C_2N_2 suggested that the α state consists of molecularly adsorbed C_2N_2, a suggestion which was supported by adsorption studies of HCN (*2*, *4*). The results of this study add further experimental evidence for this assumption. No isotopic exchange was observed in the α desorption peak and the α state can be incorporated into a saturated CO overlayer where dissociation into CN particles is inhibited for spatial reasons. Although no direct information about the bonding of α-C_2N_2 to the surface is available, indirect arguments suggest that the molecule stands "upright" at the surface, bonding occurring through the nitrogen lone pair electrons. A C_2N_2 molecule parallel to the surface would be difficult to incorporate into a c (4 × 2) CO overlayer. The similar desorption energy of CO and α-C_2N_2 (cf. Fig. 7) would also agree with the idea of similar bonding concepts for both surface species. Further, the different surface dipole with respect to the β states, where we will argue in favor of CN units parallel to the surface, would be justified.

The two β states exhibit striking differences in isotopic exchange measurements. The β_2 state shows isotopic exchange after simultaneous and consecutive exposures of C_2N_2 and $(C_2N_2)^*$. The β_1 state, however, once preformed at the surface, shows no exchange after consecutive adsorption, whereas exchange is observed during simultaneous adsorption of C_2N_2 and $(C_2N_2)^*$. Furthermore, it can be deduced that the β_1 state is populated via the β_2 state. We therefore suggest that the initial adsorption process is dissociation of C_2N_2 into CN units and the population of the β_2 state. With increasing adsorbate density association of CN units takes place forming islands of the β_1 state which grow in size as adsorption proceeds. If β_1 domains are formed by C_2N_2 preadsorption subsequent adsorption of CN* particles can only yield (CN–CN*) in the desorption process at the boundaries of the β_1 domains. During simultaneous exposure of C_2N_2 and $(C_2N_2)^*$ the resulting β_1 domains, of course, are formed by randomly distributed CN and CN* units. Desorption from the β_1 state occurs directly according to pseudo-first-order desorption kinetics with constant desorption energy as it can be expected from a somehow associated adsorbate layer. We therefore propose schematically the following adsorption–desorption sequence:

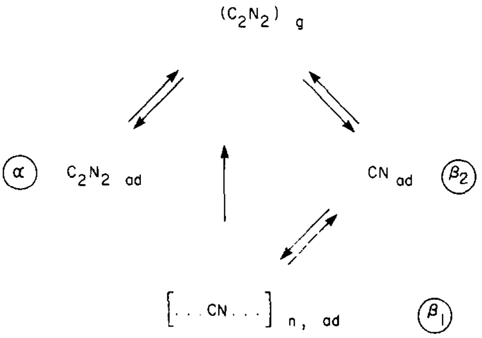

Electron spectroscopic evidence (*5–7*) and kinetic arguments (*4*) suggest multiple bonding of CN units located parallel to the surface. If the association model is valid to describe the β_1 state, parallel orientation of individual CN units with respect to the surface is required for association to take place. As to the detailed structure of the associated adsorbate layer, no information can be obtained from the present data. However, it is evident that adsorbate–adsorbate interactions will predominantly determine the formation and desorption characteristics of the associated adsorbate layer and the close correspondence of the results obtained on various Pt surfaces can therefore be rationalized.

ACKNOWLEDGMENTS

The Fonds zur Förderung der Wissenschaftlichen Forschung of Austria and the Austrian Nationalbank are acknowledged for supporting this experimental program. We are grateful to Prof. H. L. Gruber for critical discussions concerning the manuscript.

REFERENCES

1. Netzer, F. P., *Surface Sci.* **52**, 709 (1975).
2. Bridge, M. E., Marbrow, R. A., and Lambert, R. M., *Surface Sci.* **57**, 415 (1976).
3. Netzer, F. P., *Surface Sci.* **61**, 343 (1976).
4. Bridge, M. E., and Lambert, R. M., *Surface Sci.* **63**, 315 (1977); *J. Catal.* **46**, 143 (1977).
5. Conrad, H., Küppers, J., Nitschke, F., and Netzer, F. P., *Chem. Phys. Lett.* **46**, 571 (1977).
6. Wille, R. A., Netzer, F. P., and Matthew, J. A. D., *Surface Sci.* **68**, 259 (1977).
7. Conrad, H., Küppers, J., Nitschke, F., and Netzer, F. P., *J. Catal.* **52**, 186 (1978).
8. Netzer, F. P., and Wille, R. A., *Surface Sci.* **74**, 547 (1978).
9. Bertel, E., Schwaha, K., and Netzer, F. P., *Surface Sci.* **83**, 439 (1979).
10. Hoffmann, W., Masters Thesis, University of Innsbruck, 1978.
11. Redhead, P. A., *Vacuum* **12**, 203 (1962).
12. Edwards, D., Jr., *Surface Sci.* **54**, 1 (1976).
13. Ertl, G., Neumann, M., and Streit, K. M., *Surface Sci.* **64**, 393 (1977).
14. Horn, K., and Pritchard, J., *J. Phys.* **38** C4, 164 (1977).